



Squaraine-based colorimetric and fluorescent sensors for Cu²⁺-specific detection and fluorescence imaging in living cells

Weida Wang^a, Afu Fu^b, Jingsong You^{a,b}, Ge Gao^a, Jingbo Lan^{a,*}, Lijuan Chen^{b,*}

^aKey Laboratory of Green Chemistry and Technology of Ministry of Education, College of Chemistry, Sichuan University, 29 Wangjiang Road, Chengdu 610064, PR China

^bState Key Laboratory of Biotherapy, West China Hospital, West China Medical School, Sichuan University, Keyuan Road 4, Gaopeng Street, Chengdu 610041, PR China

ARTICLE INFO

Article history:

Received 4 February 2010

Received in revised form 18 March 2010

Accepted 19 March 2010

Available online 27 March 2010

Keywords:

Colorimetric chemosensor

Squaraine

Copper ion

Fluorescent probe

Imaging agents

ABSTRACT

New squaraine-based chemosensors SQ1 and SQ2 functionalized with 2-picolyl units were first synthesized and used as highly selective and sensitive colorimetric and fluorometric dual-channel sensors for Cu²⁺-specific recognition in aqueous systems. Among a series of individual metal ions, only Cu²⁺ could result in dramatic color changes. We also evaluated their capability of biological applications and found that SQ2 could be successfully employed as a Cu²⁺-selective probe in the fluorescence imaging of living cells.

© 2010 Elsevier Ltd. All rights reserved.

1. Introduction

The development of sensitive chemosensors capable of selective recognition of cations, especially for metal ions with biological interest, has always been of particular significance due to their potential application in chemistry, biomedicine, and environmental studies. The soft transition metal ion Cu²⁺ plays a pivotal part in many fundamental physiological processes as the third most abundant essential trace element after iron and zinc in the human body.¹ Research and development of chemosensors directed toward the detection and measurement of divalent copper ion has received much attention. Low level of Cu²⁺ in the cells will affect the corresponding enzyme activity, inhibit cell normal metabolism, and even endanger the survival of the cells, whereas Cu²⁺ in excess of physiological need could also cause serious diseases, for instance gastrointestinal disturbance, liver or kidney damage.^{2,3} Furthermore, Cu²⁺ can also act as a significant environmental pollutant because of its widespread use in industry and agriculture. Thus, the fast detection of Cu²⁺ in environmental and biological samples has been becoming increasingly important not only due to its important role in life but also the high toxicity to organisms under overloading conditions.⁴ Even though great achievement in the

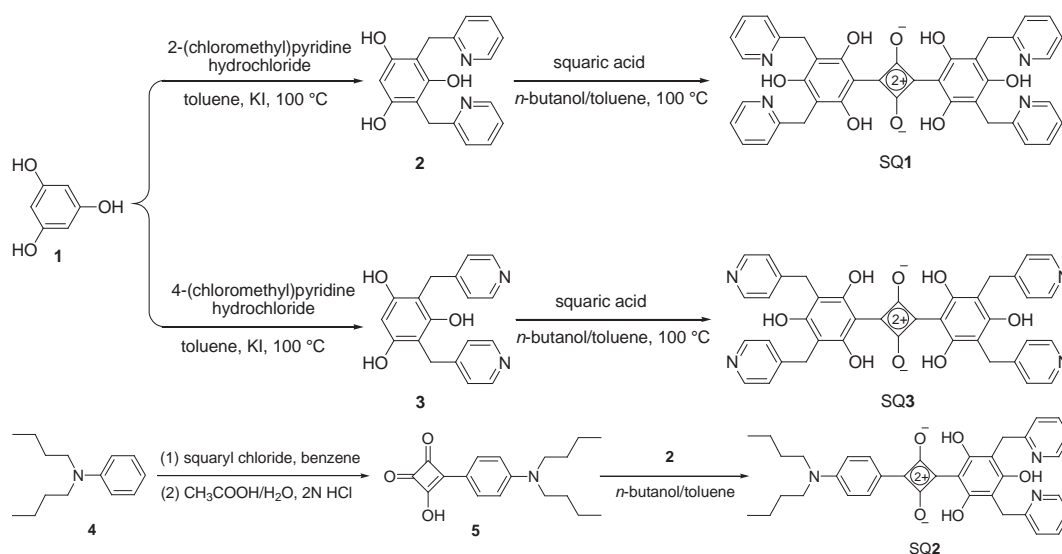
field of colorimetric and/or fluorescent chemosensors for Cu²⁺ has been obtained,⁵ there is still a demand to develop new indicators with improved properties, especially fluorescent sensors with high efficiency in the spectral visible and near-infrared (NIR) region and with specific selectivity toward Cu²⁺ over other competitive metal ions.

Squaraines are a particularly promising class of organic NIR dyes that exhibit unique photophysical properties, namely, a sharp and intense absorption band in the red to NIR region. Because their absorption and emission properties are sensitive to the surrounding medium, squaraine dyes have been designed and widely applied for the optical detection of metal ions such as Li⁺, Na⁺, Ca²⁺, Mg²⁺, Hg²⁺ in recent years.⁶ However, there are very few squaraine-based chemosensors designed for the Cu²⁺ recognition,⁷ and no studies pertaining to squaraine dyes as a versatile fluorescent scaffold for constructing bioimaging probes for Cu²⁺ so far. Therefore, the design and construction of colorimetric and fluorescent sensors based on squaraines for highly effective detection of Cu²⁺ under either in vitro or in vivo conditions is very significant.

Squaraine dyes of the type 2,4,6-trihydroxyphenylsquaraine were considered very important due to their potential application in selective recognition of specific biomolecule.⁸ However, as far as we are aware, there are very few examples⁹ on such a type of squaraine investigated because it is difficult to functionalize, especially with *N*-heterocycles. In continuation of our ongoing interest in the development of *N*-heterocycles-based supramolecular chemistry, we wish to design and construct novel 2,4,6-trihydroxyphenylsquaraine-

* Corresponding authors. Tel.: +86 28 85412285; fax: +86 28 85412203 (J.L.); tel./fax: +86 28 85164060 (J.C.); e-mail addresses: jingbolan@scu.edu.cn (J. Lan), lijuan17@hotmail.com (L. Chen).

attached chemosensors by incorporating *N*-heterocyclic groups. Inspired by the structure of DPA (di-2-pyridylmethylamine) moiety, which is well-known for the ability to sense zinc ion,¹⁰ we speculated that 2-picolyl-anchored 2,4,6-trihydroxyphenylsquaraine would provide an effective binding site for the copper ion via the synergic coordination of N and O atoms. In this context, we present the synthesis of 2,4,6-trihydroxyphenylsquaraine-derived compounds **SQ1** and **SQ2** functionalized with 2-picolyl units (**Scheme 1**) and the spectroscopic investigations upon coordination to copper(II) ion. We also present the practical applicability of **SQ2** as a fluorescent probe for the detection of Cu^{2+} in living cells. Moreover, the 2,4,6-trihydroxyphenylsquaraine-derived compound **SQ3** functionalized with 4-picolyl units was synthesized for the control experiment.



Scheme 1. Synthetic routes of squaraines **SQ1**–**SQ3**.

2. Results and discussion

2.1. Synthesis

The squaraine compound **SQ1** functionalized with 2-picolyl units was successfully synthesized by a two-step reaction with phloroglucinol and 2-(chloromethyl)pyridine hydrochloride as starting materials. Catalyzed by iodides, phloroglucinol reacted with 2-(chloromethyl)pyridine hydrochloride affording the yellow compound 2,4-bis(pyridin-2-ylmethyl)benzene-1,3,5-triol (yield 19%). The condensation of 2,4-bis(pyridin-2-ylmethyl)benzene-1,3,5-triol and squaric acid in toluene and *n*-butanol (*v/v*=1:1) gave rise to **SQ1** (yield 78%). The unsymmetrical squaraine derivative **SQ2** was prepared by the reaction of 3-[4-(*N,N*-dibutylamino)phenyl]-4-hydroxycyclobutene-1,2-dione with 2,4-bis-(pyridin-2-ylmethyl)benzene-1,3,5-triol (yield 60%). To understand a crucial role which 2-picolyl unit played as a binding site for Cu^{2+} , we synthesized the compound **SQ3** bearing 4-picolyl units on the phloroglucinol moiety via a similar synthetic route as **SQ1**.

2.2. Colorimetric assay of **SQ1**

A small amount of chemosensor **SQ1** is soluble in a mixed solvent of 10 mM HEPES solution and THF (*v/v*=60/40, pH=7.4), and further diluted for analyte detection. **Figure 1** showed the color changes of **SQ1** (10 μM) upon addition of 1.0 equiv of a series of individual metallic cations including Li^+ , Na^+ , K^+ , Ca^{2+} , Sr^{2+} , Ba^{2+} ,

Mg^{2+} , Fe^{3+} , Co^{2+} , Ni^{2+} , Cu^{2+} , Zn^{2+} , Cr^{3+} , Cd^{2+} , Pb^{2+} , Mn^{2+} , Hg^{2+} , Ag^+ , La^{3+} , Ce^{3+} , Pr^{3+} , Nd^{3+} , Y^{3+} , Er^{3+} , Sm^{3+} , Gd^{3+} , and Sc^{3+} ions. As depicted in **Figure 1**, a 10^{-5} M solution of **SQ1** displayed a strong pink color and Cu^{2+} caused a dramatic change of color from pink to blue while other metal cations did not result in appreciable changes under the same condition. The fact indicated the compound **SQ1** exhibited a high selectivity for Cu^{2+} over various other metal ions. The limit of Cu^{2+} by naked eye was 3 μM (**Fig. S1 in the Supplementary data**), which was far lower than the limit of Cu^{2+} in drinking water (~ 20 μM) set by the U.S. Environmental Protection Agency (EPA). Therefore, the advantage of this assay is that naked-eye detection of Cu^{2+} in water quality monitoring becomes possible. Moreover, to explore the effects of anionic counterions on the sensing behavior, the responses of **SQ1** to different cupric salts



Figure 1. (left) The color changes of **SQ1** ($c=10$ μM) in (10 mM) HEPES/THF (*v/v*=60/40, pH=7.4) upon addition of 1.0 equiv of various metal ions. From left to right and top to bottom: Li^+ , Na^+ , K^+ , Ca^{2+} , Mg^{2+} , Sr^{2+} , Ba^{2+} , Fe^{3+} , Co^{2+} , Ni^{2+} , Cu^{2+} , Zn^{2+} , Cr^{3+} , Cd^{2+} , Mn^{2+} , Pb^{2+} , Hg^{2+} , Ag^+ , La^{3+} , Ce^{3+} , Pr^{3+} , Nd^{3+} , Y^{3+} , Er^{3+} , Sm^{3+} , Gd^{3+} , Sc^{3+} , blank. (right) Schematic representation of the periodic table of metallic elements.

were also studied. As we expected, cupric bromide, cupric sulfate, and cupric acetate could result in the same color change as cupric chloride (**Fig. S2**). The further research revealed that the color changes of **SQ1** induced by Cu^{2+} were reversible as the addition of EDTA reversed the color changes.

2.3. Spectral investigations of **SQ1**

The spectral responses of **SQ1** (10 μM) to a range of physiological and environmentally relevant metal ions were depicted in **Figure 2**. **SQ1** had a very strong absorption band centered at 514 nm. The UV-vis absorption spectrum of **SQ1** solution shifted largely to the red about 161 nm when combined with Cu^{2+} , but no significant spectral changes were observed when combined with other metals, which probably attributed to their lower affinity with the receptor **SQ1**. In particular, in the competitive experiment of **SQ1**, the

existence of alkali, alkaline earth, and other transition metal ions did not interfere with the recognition of Cu^{2+} , which indicated that SQ1 was potentially applicable to the Cu^{2+} sensing in complicated environmental samples (Fig. 2).

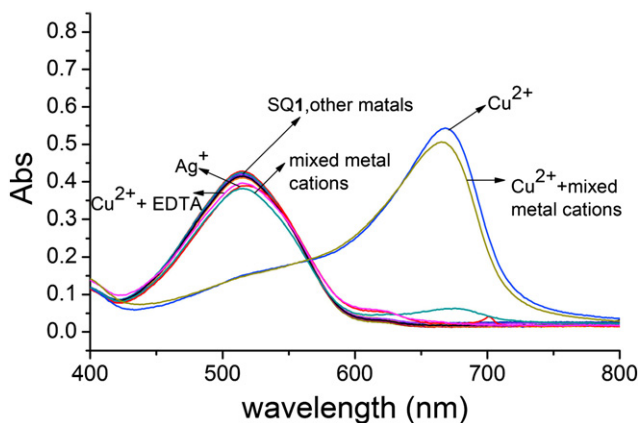


Figure 2. UV-vis absorption changes of SQ1 (10 μM) in (10 mM) HEPES/THF (v/v=60/40, pH=7.4) in the presence of 1 equiv of different chloride salts (except for mercuric acetate and silver nitrate) including Li^+ , Na^+ , K^+ , Ca^{2+} , Mg^{2+} , Fe^{3+} , Co^{2+} , Ni^{2+} , Cu^{2+} , Zn^{2+} , Cr^{3+} , Cd^{2+} , Pb^{2+} , Mn^{2+} , Hg^{2+} , Ag^+ , and their mixture.

To understand the coordination behavior between SQ1 and Cu^{2+} , the UV-vis absorption spectral titration experiment of SQ1 with Cu^{2+} in (10 mM) HEPES/THF (v/v=60/40, pH=7.4) was carried out. As shown in Figure 3a, the original absorption band centered at 514 nm gradually decreased in intensity upon addition of Cu^{2+} with the formation of a new absorption band at ca. 675 nm, generating an isosbestic point at 565 nm, which indicated a new complex was formed. The Job's plot of the UV-vis titrations revealed a 1:1 stoichiometric ratio between the Cu^{2+} ion and SQ1 (Fig. 3b). The ESI-TOF mass spectrum of a mixture of SQ1 and CuCl_2 also revealed the formation of a 1:1 metal-ligand complex through the metal coordination interaction where there was a major signal at m/z 787.25 (calcd 787.15) assigned to the species $[\text{SQ1}(\text{Cu})\cdot\text{CH}_3\text{OH}-2\text{H}]^+$ (Fig. S13). The stability constant of the newly formed complex was determined as $1.9 \times 10^6 \text{ M}^{-1}$ ($R=0.993$) by using nonlinear curve fitting (Fig. S3).¹¹

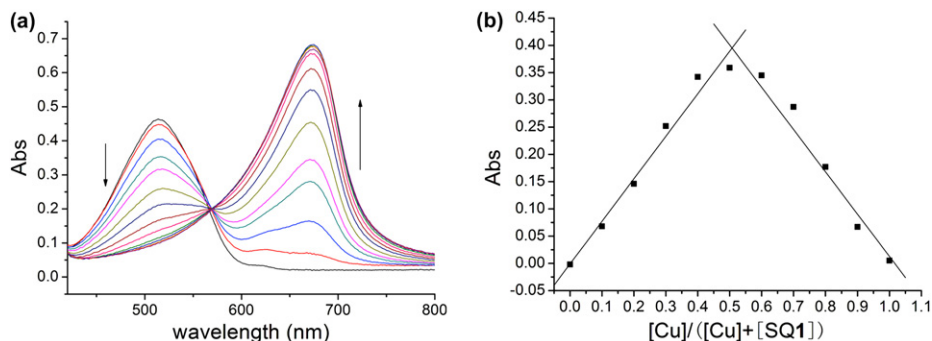


Figure 3. (a) UV-vis titration curves (0–1.3 equiv) and (b) Job plot analysis of a solution of SQ1 in (10 mM) HEPES/THF (v/v=60/40, pH=7.4) with Cu^{2+} .

The selectivity of SQ1 to Cu^{2+} ion was further investigated by fluorometric detection in HEPES/THF (v/v=60/40, pH=7.4). Chemosensor SQ1 exhibited a relative strong fluorescence emission at 626 nm upon excitation at 530 nm. Upon addition of the same amount of various metal ions, only Cu^{2+} quenched nearly 85 percent fluorescent intensity of SQ1, and no new emission emerged. Compound SQ1 did not respond distinctly to other metal species. The obvious selectivity of SQ1 toward Cu^{2+} suggested that SQ1 could be used as a fluorescent probe in sensing Cu^{2+} (Fig. 4). We had intended

to further evaluate the capability of SQ1 as a fluorescent probe to image Cu^{2+} in living cells. Unfortunately, SQ1 could not dissolve in cell cultured medium and even in D-Hanks containing 1% DMSO.

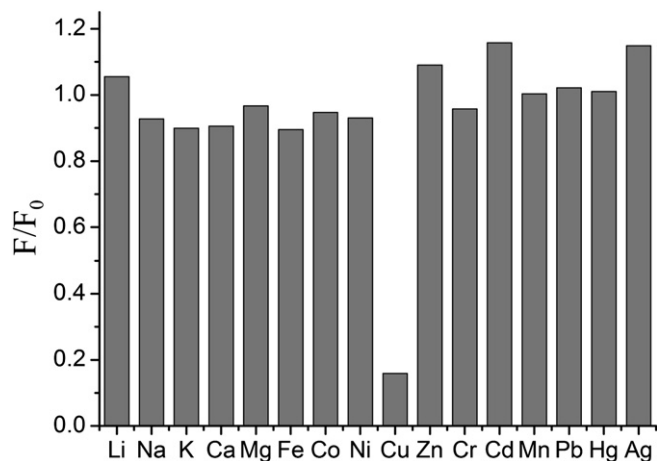


Figure 4. Fluorescent responses of SQ1 ($C=10 \mu\text{M}$) in (10 mM) HEPES/THF (v/v=60/40, pH=7.4) to various metal ions (1 equiv). Excitation was at 530 nm and emission was at 626 nm.

To understand a crucial role, which 2-picoyl unit played on the sensing behavior, we synthesized squaraine-based derivative SQ3 bearing 4-picoyl units and investigated the responses of SQ3 to Cu^{2+} under the same condition as SQ1. As depicted in Figures S4 and S5, Cu^{2+} induced no appreciable absorption or fluorescence spectral changes revealing that SQ3 had lower affinity for Cu^{2+} compared with SQ1. The assay indicated that the nitrogen atom on the 2-position of the pyridine group acted as an important binding site for the Cu^{2+} complexation.

2.4. The proposed binding model

The binding model of SQ1 and Cu^{2+} proposed was illustrated in Figure 5. Cu^{2+} was coordinated by the phenolic hydroxyl oxygen atom and two 2-picoyl nitrogen atoms in a three-dimensional way. For squaraine SQ1, resonance-stabilized zwitterionic structure was

preferred, while the binding of Cu^{2+} might localize the positive charge to the phenolic hydroxyl group, which was opposite to the Cu^{2+} -complexed binding site.¹² On the basis of this hypothesis, the symmetrical squaraine SQ1 could only bind one copper ion which was consistent with the 1:1 stoichiometry between SQ1 and Cu^{2+} from Job plot analysis. The importance of 2-picoyl groups was that they provided additional synergic coordination sites for effective Cu^{2+} recognition, which was supported by the comparative experiment between SQ1 and SQ3.

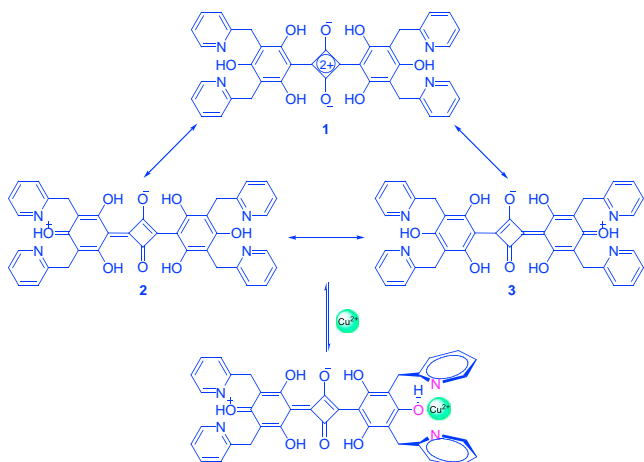


Figure 5. The proposed charge-localized mechanism of sensing Cu^{2+} .

2.5. Selectivity of SQ2 to Cu^{2+}

Fluorescent sensors that can selectively monitor specific metal ions in living cells have been indispensable tools for understanding of biological phenomena. Considering the proper amphiphaticity of a sensor was favorable for cellular uptake and intracellular fluorescent imaging,¹³ we also prepared the 2,4,6-trihydroxyphenylsquaraine-based compound SQ2 with two butyl chains. We studied the responses of SQ2 (10 μM) to various metals in (10 mM) HEPES/THF ($v/v=60/40$, $\text{pH}=7.4$) and it was proved to be a colorimetric probe for Cu^{2+} with high selectivity and sensitivity as SQ1 (Fig. S6). A solution of SQ2 (10 μM) displayed a bright purple color and the color turned blue-black upon addition of 1.0 equiv of Cu^{2+} , while the same amount of other metallic ions did not interfere with the Cu^{2+} detection by naked eye. The limit of Cu^{2+} by naked eye was as low as SQ1 (Fig. S7) and anionic counterions had no effect on the sensing behavior (Fig. S8).

The spectral responses of SQ2 (10 μM) to a range of physiological and environmentally relevant metal ions were depicted in Figure 6. As depicted in Figure 6, a strong absorption band peaked at 554 nm was observed and there was a large 86 nm red shift upon addition of Cu^{2+} ,

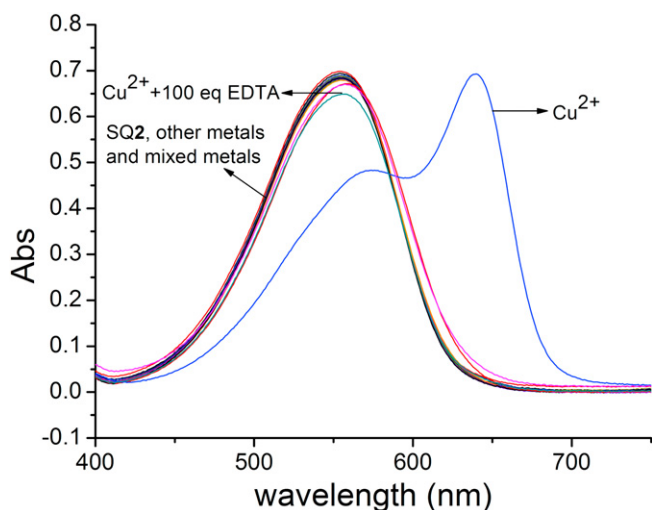


Figure 6. UV-vis absorption changes of SQ2 (10 μM) in (10 mM) HEPES/THF ($v/v=60/40$, $\text{pH}=7.4$) in the presence of 1 equiv of different chloride salts (except for mercuric acetate and silver nitrate) including Li^+ , Na^+ , K^+ , Ca^{2+} , Mg^{2+} , Fe^{3+} , Co^{2+} , Ni^{2+} , Cu^{2+} , Zn^{2+} , Cr^{3+} , Cd^{2+} , Pb^{2+} , Mn^{2+} , Hg^{2+} , and Ag^+ .

but no significant spectral changes were observed when other competing metals were added. The UV-vis titration curves did not change obviously any more (Fig. S9) and the absorption band peaked at 640 nm arrived at the maximum value (Fig. S10) after addition of 1 equiv of Cu^{2+} indicating the 1:1 complexation of SQ2 and Cu^{2+} . The 1:1 stoichiometry was further confirmed by the electrospray ionization (ESI) mass spectrum analysis (Fig. S14). ESI-TOF mass spectroscopy showed a peak at $m/z=737.33$ for $[\text{SQ2}(\text{Cu})\cdot 2\text{CH}_3\text{OH}\cdot \text{H}_2\text{O}+\text{H}]^+$ (calcd 737.27). The related experimental results and figures were displayed in the Supplementary data.

To evaluate the possibility of SQ2 as a fluorescent probe to image Cu^{2+} in living cells, we first examined the selectivity of SQ2 (10 μM) to Cu^{2+} ion by fluorometric detection in DMSO/Hanks ($v/v=40/60$, $\text{pH}=7.0$). As shown in Figure 7 and Figure S12, only Cu^{2+} quenched nearly 90 percent fluorescent intensity of SQ2, while other biologically relevant metal cations did not induce any discernible changes in emission intensities. The high selectivity of SQ2 to Cu^{2+} clearly established that SQ2 had the potential application of serving as a fluorescent probe for live-cell imaging.

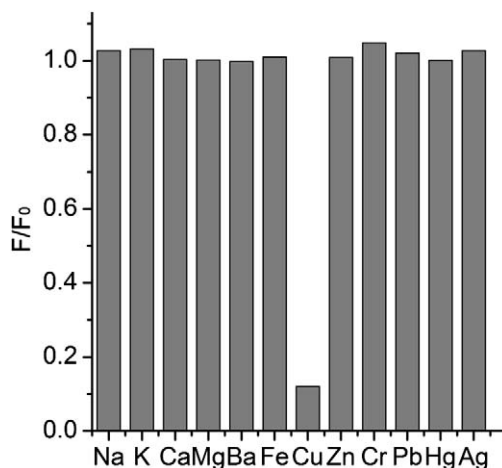


Figure 7. Fluorescent responses of SQ2 (10 μM) in DMSO/Hanks ($v/v=40/60$, $\text{pH}=7.0$) to various metals (1 equiv) with excitation at 550 nm and emission at 651 nm (emission slits=3 nm).

2.6. Cell imaging and cytotoxicity assay

To determine whether SQ2 could be used as a Cu^{2+} probe in living cells, we carried out experiments on LL/2 and HepG2 cells with SQ2. After LL/2 and HepG2 cells were cultured in D-Hanks buffer containing 1% DMSO supplemented with 20 μM SQ2 at 37 $^\circ\text{C}$ for 1 h and 0.5 h, respectively and washed with D-Hanks buffer to remove the remaining dye SQ2, a clear red fluorescent image could be observed obviously from fluorescence microscopy as shown in Figure 8. The intracellular fluorescence became faint after addition of Cu^{2+} (5 equiv) and was effectively restored by addition of EDTA. The experimental results revealed that SQ2 permeated well through the cell membrane and could be used as a fluorescent probe for imaging labile Cu^{2+} in living biological samples. Subsequently, visualization of localization within live LL/2 cells and HepG2 cells was determined using a confocal laser scanning microscopy (CLSM). As demonstrated in Figure 9, the squaraine SQ2 preferentially accumulated in the cytoplasm, and especially around the perinuclear region. To evaluate cytotoxicity of the probe, SQ2 was taken as an example to perform a MTT assay on HepG2 cells with dye concentrations from 5 μM to 20 μM . The cellular viability estimated was ca. 66% in 24 h after treatment with 20 μM of SQ2 (Fig. 10), exhibiting low toxicity to cultured cells.

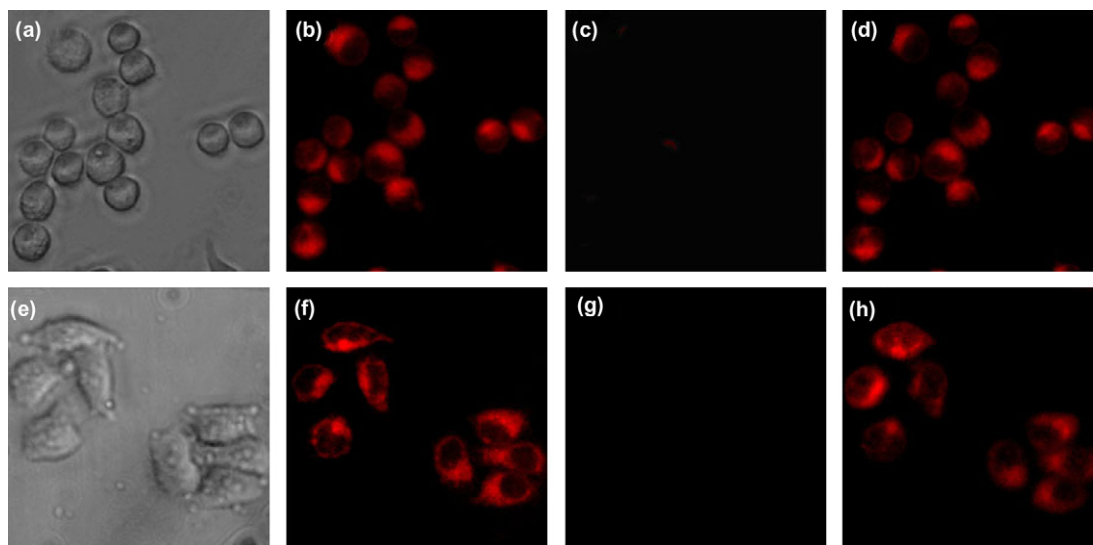


Figure 8. Brightfield and fluorescence images of LL/2 (a–d) and HepG2 (e–h) cells. (a,e) Brightfield images of LL/2 and HepG2 cells; (b,f) fluorescence images of LL/2 and HepG2 cells stained with 20 μM SQ2 at 37 $^{\circ}\text{C}$ for 1 h and 0.5 h, respectively; (c,g) Further supplemented with addition of CuCl_2 (100 μM); (d,h) return of fluorescence after addition of EDTA (500 μM).

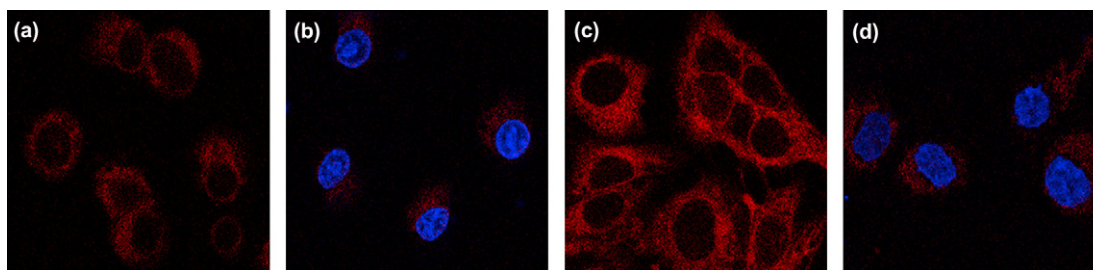


Figure 9. CLSM images of (a,b) LL/2 cells and (c,d) HepG2 cells treated with SQ2 and Hoechst 33258 (cell nuclei stained) in D-Hanks buffer containing 1% DMSO for 30 min.

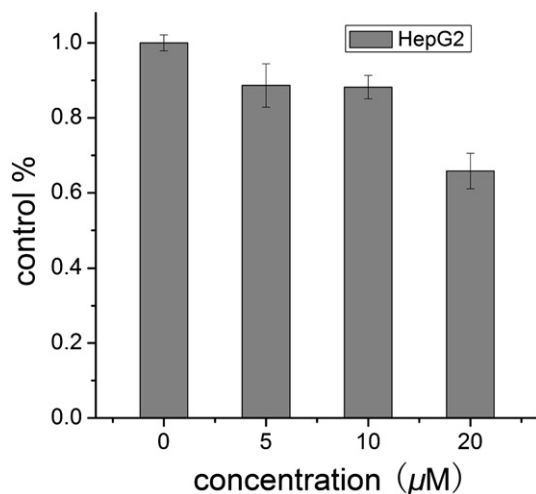


Figure 10. Cell viability values (%) estimated by a MTT assay on HepG2 cells.

3. Conclusion

In conclusion, we have developed highly sensitive and selective colorimetric and fluorometric dual-channel sensors SQ1 and SQ2 for Cu^{2+} in aqueous solution. The two colorimetric probes can make 'naked-eye' detection of Cu^{2+} in the visible wavelength region.

Colorimetric methods can be convenient in practical applications without the aid of any advanced instruments. Especially, the chemosensor SQ2 can be employed as a Cu^{2+} -selective probe in the fluorescence imaging of living cells. Such a sensor would become valuable in revealing the roles of Cu^{2+} in biological systems under either in vitro or in vivo conditions.

4. Experimental

4.1. General

^1H NMR and ^{13}C NMR spectra were recorded on a Bruker AV-400 (^1H : 400 MHz; ^{13}C : 100 MHz) or a Varian INOVA-400 (^1H : 400 MHz; ^{13}C : 100 MHz). The ^1H NMR (400 MHz) chemical shifts were measured relative to TMS (0.00 ppm) for CDCl_3 or relative to $\text{DMSO}-d_6$ as indicated. The ^{13}C NMR (100 MHz) chemical shifts were given relative to $\text{DMSO}-d_6$ and CDCl_3 as indicated. High resolution mass spectra (HRMS) were recorded on a Waters-TOF Premier Mass Spectrometer by positive ESI-Q-TOF. Absorption spectra were detected on a HITACHI U-2910 spectrometer. Fluorescent emission spectra were collected on a Horiba Jobin Yvon-Edison Fluoromax-4 fluorescence spectrometer. Melting points of compounds were determined with XRC-1 and were uncorrected. Unless otherwise noted, all chemicals and reagents were obtained from commercial suppliers and used without further purification. *n*-Butanol was dried by heating at reflux over sodium and distilled prior to use. Benzene or toluene was treated firstly by shaking with concd H_2SO_4 until free form thiophene, then washed with water,

dilute NaOH, and water, followed by drying with sodium, and distilled prior to use. All syntheses and manipulations were carried out under dry N₂ atmosphere. The stock solutions of fluorophores and metal chloride were freshly prepared and used for each measurement. THF was either HPLC or spectroscopic grade and water was distilled for twice. Each time a 3 mL of receptor solution was filled in a quartz cell of 1 cm of optical path length, and the stock solution of metal chloride was added into a quartz cell dropwise using a micro-syringe. The volume of metal chloride stock solution added was less than 100 µL to remain the concentration of receptor unchanged. The excitation and emission slits of fluorescence spectra were set at 5.0 nm if not specified.

4.2. Synthesis of 2,4-bis(pyridin-2-ylmethyl)benzene-1,3,5-triol (2)

A mixture of 2-(chloromethyl)pyridine hydrochloride (4.0 g, 24.4 mmol), anhydrous phloroglucinol (1.0 g, 8.0 mmol), and potassium iodide (0.1 g) in 8 mL of toluene was heated at 100 °C with stirring under nitrogen for 24 h and then cooled to ambient temperature, followed by addition of methanol (16 mL), dichloromethane (16 mL), and sodium hydrogen carbonate (5.0 g, 59.5 mmol). The mixture was allowed to stir overnight at room temperature. The resulting mixture was then filtered and washed well with methanol (15 mL) and dichloromethane (15 mL). The filtrate was concentrated under reduced pressure. The residue was purified by column chromatography on silica gel eluting with ethyl acetate/dichloromethane (1/6) to afford a slightly yellow product (0.47 g, yield 19%). Mp: 193–195 °C. ¹H NMR (400 MHz, DMSO-*d*₆): δ=3.96 (s, 4H), 6.00 (s, 1H), 7.16 (d, *J*=7.6 Hz, 2H), 7.20–7.23 (m, 2H), 7.68–7.72 (m, 2H), 8.43–8.44 (m, 2H), 9.30 (s, 2H), 10.73 (s, 1H) ppm. ¹³C NMR (100 MHz, DMSO-*d*₆): δ=31.9, 95.3, 105.1, 121.6, 122.4, 137.7, 148.2, 154.8, 155.8, 161.9 ppm. HRMS (ESI): *m/z* calcd for C₁₈H₁₇N₂O₃ [M+H]⁺ 309.1239, found 309.1231.

4.3. Synthesis of SQ1

A flame-dried Schlenk test tube with a magnetic stirring bar was charged with squaric acid (0.008 g, 0.074 mmol), 2,4-bis(pyridin-2-ylmethyl)benzene-1,3,5-triol (0.045 g, 0.147 mmol), toluene (4.5 mL), and *n*-butanol (4.5 mL) under nitrogen. The reaction mixture was heated at 100 °C with stirring for 20 h and then cooled to ambient temperature. The resulting mixture was filtered and the solid was washed with isopropanol and hexane until the filtrate was almost colorless. The desired product was obtained as a purple solid (40 mg, yield 78%). Mp: >300 °C. ¹H NMR (400 MHz, DMSO-*d*₆): δ=4.06 (s, 4H), 4.14 (s, 4H), 7.42 (d, *J*=8.0 Hz, 2H), 7.49–7.55 (m, 4H), 7.57–7.60 (m, 2H), 8.04 (t, *J*=6.8 Hz, 2H), 8.10 (t, *J*=8.0 Hz, 2H), 8.58 (d, *J*=4.8 Hz, 2H), 8.61 (d, *J*=5.2 Hz, 2H) 12.36 (s, 2H) ppm. ¹³C NMR data were not recorded due to poor solubility. HRMS (ESI): *m/z* calcd for C₄₀H₃₁N₄O₈ [M+H]⁺ 695.2142, found 695.2136.

4.4. Synthesis of 2,4-bis(pyridin-4-ylmethyl)benzene-1,3,5-triol (3)

A mixture of 4-(chloromethyl)pyridine hydrochloride (4.0 g, 24.4 mmol), anhydrous phloroglucinol (1.0 g, 8.0 mmol), and potassium iodide (0.1 g) in 8 mL of toluene was heated at 100 °C with stirring under nitrogen for 12 h and then cooled to ambient temperature, followed by addition of methanol (16 mL), dichloromethane (16 mL), and sodium hydrogen carbonate (5.0 g, 59.5 mmol). The mixture was allowed to stir overnight at room temperature. The resulting mixture was then filtered and washed well with methanol (15 mL) and dichloromethane (15 mL). The filtrate was concentrated under reduced pressure. The residue was purified by column chromatography on silica gel eluting with

methanol/ethyl acetate (1/7) to afford a yellow product (0.78 g, yield 32%). Mp: 148–150 °C. ¹H NMR (400 MHz, DMSO-*d*₆): δ=3.84 (s, 4H), 6.06 (s, 1H), 7.12 (d, *J*=6.0 Hz, 4H), 8.34 (s, 1H), 8.36–8.38 (m, 4H), 9.16 (s, 2H) ppm. ¹³C NMR (100 MHz, DMSO-*d*₆): δ=28.2, 95.0, 104.6, 123.9, 149.2, 151.6, 154.6, 155.0 ppm. HRMS (ESI): *m/z* calcd for C₁₈H₁₇N₂O₃ [M+H]⁺ 309.1239, found 309.1235.

4.5. Synthesis of SQ3

A flame-dried Schlenk test tube with a magnetic stirring bar was charged with squaric acid (0.013 g, 0.11 mmol), 2,4-bis(pyridin-4-ylmethyl)benzene-1,3,5-triol (0.070 g, 0.23 mmol), toluene (5 mL), and *n*-butanol (5 mL) under nitrogen. The reaction mixture was stirred at reflux for 57 h and then cooled to ambient temperature. The resulting mixture was filtered and the solid was washed with isopropanol and hexane until the filtrate was almost colorless. The desired product was obtained as a purple solid (31 mg, yield 41%). Mp: >300 °C. ¹H NMR (400 MHz, DMSO-*d*₆): δ=3.97 (s, 8H), 6.09 (s, 2H), 6.57 (br s, 4H), 7.44 (d, *J*=5.2 Hz, 8H), 8.56 (d, *J*=4.8 Hz, 8H) ppm. ¹³C NMR (100 MHz, DMSO-*d*₆): δ=28.9, 95.1, 103.9, 125.2, 145.2, 154.6, 155.3, 157.6, 195.7 ppm. HRMS (ESI): *m/z* calcd for C₄₀H₂₉N₄O₈ [M-H]⁺ 693.1985, found 693.1984.

4.6. Synthesis of *N,N*-dibutylbenzenamine (4)

A sodium hydroxide solution (20 mL, 8 N) was added dropwise to a stirred mixture of 1-bromobutane (15 mL, 0.16 mol) and aniline (5 mL, 53.69 mmol) at 100 °C under nitrogen and the reaction mixture was continued to react for 48 h. After being cooled to ambient temperature, the resulting mixture was extracted with ethyl acetate and the combined extracts were dried over anhydrous sodium sulfate. The obtained organic layer was concentrated under reduced pressure and the residue was purified by column chromatography on silica gel eluting with petroleum ether/dichloromethane (1/1) to afford a yellow liquid (8 g, yield 73%). ¹H NMR (400 MHz, CDCl₃): δ=1.04 (t, *J*=7.6 Hz, 6H), 1.41–1.50 (m, 4H), 1.63–1.71 (m, 4H), 3.34 (t, *J*=7.6 Hz, 4H), 6.70–6.76 (m, 3H), 7.28–7.32 (m, 2H) ppm. HRMS (ESI): *m/z* calcd for C₁₄H₂₄N [M+H]⁺ 206.1909, found 206.1906.

4.7. Synthesis of 3-[4-(*N,N*-dibutylamino)phenyl]-4-hydroxycyclobutene-1,2-dione^{6e,14} (5)

A solution of *N,N*-dibutylbenzenamine (1.36 g, 6.62 mmol) in dried benzene (30 mL) was added to a round flask charged with squaryl chloride (1.0 g, 6.62 mmol) prepared following the reported procedure¹⁵ and refluxed for 15 h. The resulting mixture was then cooled to ambient temperature, dissolved in a mixture of acetic acid (25 mL), water (25 mL), and concentrated HCl (1.3 mL) and refluxed for 3 h. After being cooled to ambient temperature, the yellow precipitate was obtained by filtration, washed with ether, and dried (yield 71%). ¹H NMR (400 MHz, DMSO-*d*₆): δ=0.88 (t, *J*=7.2 Hz, 6H), 1.27–1.36 (m, 4H), 1.49 (s, 4H), 3.39 (s, 4H), 4.94 (br s, 1H), 6.87 (s, 2H), 7.86 (s, 2H) ppm. HRMS (ESI): *m/z* calcd for C₁₈H₂₃NO₃Na [M+Na]⁺ 324.1576, found 324.1573.

4.8. Synthesis of SQ2

A flame-dried Schlenk test tube with a magnetic stirring bar was charged with compound **2** (0.102 g, 0.33 mmol), compound **5** (0.100 g, 0.33 mmol), toluene (8 mL), and *n*-butanol (8 mL) under nitrogen. The reaction mixture was stirred at reflux for 34 h and then cooled to ambient temperature. The solvent was removed under reduced pressure and the residue was purified by column chromatography on silica gel eluting with methanol/dichloromethane (1/20) to afford a blue solid (0.12 g, yield 60%). Mp: 134–

136 °C. ^1H NMR (400 MHz, CDCl_3): δ =0.92–0.99 (m, 6H), 1.33–1.42 (m, 4H), 1.58–1.65 (m, 4H), 3.36 (t, J =7.6 Hz, 4H), 4.07 (s, 4H), 6.67 (d, J =8.8 Hz, 2H), 7.07 (s, 2H), 7.41 (s, 2H), 7.62 (s, 2H), 8.05 (d, J =8.0 Hz, 2H), 8.34 (s, 2H), 12.93 (s, 3H) ppm. ^{13}C NMR (100 MHz, CDCl_3): δ =13.8, 20.2, 29.5, 31.4, 51.1, 108.1, 108.7, 112.3, 117.6, 121.4, 123.5, 132.3, 137.8, 147.4, 160.9, 161.4, 182.9 ppm. HRMS (ESI): m/z calcd for $\text{C}_{36}\text{H}_{38}\text{N}_3\text{O}_5$ $[\text{M}+\text{H}]^+$ 592.2811, found 592.2803.

4.9. Cell culture

Human hepatocellular carcinoma cell line HepG2 and Lewis lung carcinoma cell line LL/2 were obtained from the American Type Culture Collection (ATCC) and cultured in DMEM containing 10% fetal bovine serum (FBS), 100 IU/mL penicillin, and 100 $\mu\text{g}/\text{mL}$ streptomycin. All cells were incubated in an atmosphere of 5% CO_2 at 37 °C.

4.10. Fluorescence images

HepG2 and LL/2 Cells (2×10^4 /well) were plated into 24-well plates. After 24 h, Cells were loaded with SQ2 by incubation in D-Hanks buffer (140 mM NaCl, 2.8 mM KCl, 1 mg/ml glucose, 0.44 mM KH_2PO_4 , 0.37 mM Na_2HPO_4 , pH=7.0) at 37 °C for 0.5 h or 1 h and washed with D-Hanks buffer to remove the remaining dye SQ2. Fluorescence was then examined under a fluorescence microscopy (Zeiss Axiovert 200) irradiated by green light source (540–580 nm).

Confocal fluorescence imaging was performed with a Leica TCS SP2 confocal laser scanning microscope and a 60 \times oil-immersion objective lens. Excitation of SQ2-loaded cells at 543 nm was carried out with a HeNe laser. Excitation of Hoechst 33258-loaded cells at 405 nm was carried out with a semiconductor laser.

4.11. Cytotoxicity assay

3-(4,5-Dimethylthiazol-2-yl)-2,5-diphenyltetrazolium bromide (MTT) assay were performed to evaluate the cytotoxicity effect of SQ2. HepG2 cells were incubated in a 96-well culture plates at a volume of 100 μL (5×10^4 cells/mL) for a stationary culture. The media were changed into fresh media with a final volume of 200 μL containing SQ2 in the 2-fold down dilution series and then incubated for 24 h. The control culture was treated with DMSO. Then 20 μL of MTT (5 mg/mL in PBS) was added to each well, incubated for an additional 4 h. After centrifuged at 1000 rpm for 5 min, the medium was removed. MTT formazan precipitate was dissolved in 150 μL of DMSO, shaken mechanically for 5 min and then absorbance readings at a wavelength of 570 nm were taken on a spectrophotometer (Molecular Devices, Sunnyvale, USA). The cell viability was calculated by the following formula: (mean optical density (OD) in treated wells/mean OD in control wells) $\times 100\%$.

Acknowledgements

This work was supported by grants from the National Natural Science Foundation of China (No. 20772086). We thank the Centre of Testing and Analysis, Sichuan University for NMR measurements.

Supplementary data

Supplementary data associated with this article can be found in online version at doi:10.1016/j.tet.2010.03.070. These data include MOL files and InChiKeys of the most important compounds described in this article.

References and notes

- (a) Linder, M. C.; Hazegh-Azam, M. *Am. J. Clin. Nutr.* **1996**, *63*, 797S–811S; (b) Uauy, R.; Olivares, M.; Gonzalez, M. *Am. J. Clin. Nutr.* **1998**, *67*, 952S–959S.
- Krämer, R. *Angew. Chem., Int. Ed.* **1998**, *37*, 772–773.
- Georgopoulos, P. G.; Roy, A.; Yonone-Lioy, M. J.; Opiekun, R. E.; Lioy, P. J. *J. Toxicol. Environ. Health, B* **2001**, *4*, 341–394.
- Zhou, Y.; Wang, S.; Zhang, K.; Jiang, X. *Angew. Chem., Int. Ed.* **2008**, *47*, 7454–7456.
- (a) Jung, H. S.; Kwon, P. S.; Lee, J. W.; Kim, J. I.; Hong, C. S.; Kim, J. W.; Yan, S.; Lee, J. Y.; Lee, J. H.; Joo, T.; Kim, J. S. *J. Am. Chem. Soc.* **2009**, *131*, 2008–2012; (b) Huang, J.; Xu, Y.; Qian, X. *Org. Biomol. Chem.* **2009**, *7*, 1299–1303; (c) Zhou, Y.; Wang, F.; Kim, Y.; Kim, S.-J.; Yoon, J. *Org. Lett.* **2009**, *11*, 4442–4445; (d) Zhao, Y.; Zhang, X.-B.; Han, Z.-X.; Qiao, L.; Li, C.-Y.; Jian, L.-X.; Shen, G.-L.; Yu, R.-Q. *Anal. Chem.* **2009**, *81*, 7022–7030; (e) Zeng, L.; Miller, E. W.; Pralle, A.; Isacoff, E. Y.; Chang, C. J. *J. Am. Chem. Soc.* **2006**, *128*, 10–11; (f) Martinez, R.; Zapata, F.; Caballero, A.; Espinosa, A.; Trraga, A.; Molina, P. *Org. Lett.* **2006**, *8*, 3235–3238; (g) Zhang, X.; Shiraishi, Y.; Hirai, T. *Org. Lett.* **2007**, *9*, 5039–5042; (h) Kim, H. J.; Hong, J.; Hong, A.; Ham, S.; Lee, J. H.; Kim, J. S. *Org. Lett.* **2008**, *10*, 1963–1966; (i) Sheng, R.; Wang, P.; Gao, Y.; Wu, Y.; Liu, W.; Ma, J.; Li, H.; Wu, S. *Org. Lett.* **2008**, *10*, 5015–5018; (j) Guo, Z.; Zhu, W.; Tian, H. *Macromolecules* **2010**, *43*, 739–744; (k) Xu, Z.; Pan, J.; Spring, D. R.; Cui, J.; Yoon, J. *Tetrahedron* **2010**, *66*, 1678–1683.
- (a) Chenthamarakshan, C. R.; Eldo, J.; Ajayaghosh, A. *Macromolecules* **1999**, *32*, 5846–5851; (b) Hsueh, S.-Y.; Lai, C.-C.; Liu, Y.-H.; Peng, S.-M.; Chiu, S.-H. *Angew. Chem., Int. Ed.* **2007**, *46*, 2013–2017; (c) Hsueh, S.-Y.; Lai, C.-C.; Liu, Y.-H.; Wang, Y.; Peng, S.-M.; Chiu, S.-H. *Org. Lett.* **2007**, *9*, 4523–4526; (d) Akkaya, E. U.; Turkyilmaz, S. *Tetrahedron Lett.* **1997**, *38*, 4513–4516; (e) Arunkumar, E.; Chithra, P.; Ajayaghosh, A. *J. Am. Chem. Soc.* **2004**, *126*, 6590–6598; (f) Arunkumar, E.; Ajayaghosh, A.; Daub, J. *J. Am. Chem. Soc.* **2005**, *127*, 3156–3164; (g) Yagi, S.; Hyodo, Y.; Hirose, M.; Nakazumi, H.; Sakurai, Y.; Ajayaghosh, A. *Org. Lett.* **2007**, *9*, 1999–2002; (h) Ros-Lis, J. V.; Martínez-Mañez, R.; Rurack, K.; Sancenón, F.; Soto, J.; Spieles, M. *Inorg. Chem.* **2004**, *43*, 5183–5185; (i) Ros-Lis, J. V.; Marcos, M. D.; Martínez-Mañez, R.; Rurack, K.; Soto, J. *Angew. Chem., Int. Ed.* **2005**, *44*, 4405–4407; (j) Basheer, M. C.; Alex, S.; Thomas, K. G.; Suresh, C. H.; Das, S. *Tetrahedron* **2006**, *62*, 605–610.
- Chandrasekaran, Y.; Dutta, G. K.; Kanth, R. B.; Patil, S. *Dyes Pigm.* **2009**, *83*, 162–167.
- Jisha, V. S.; Arun, K. T.; Hariharan, M.; Ramaiah, D. *J. Am. Chem. Soc.* **2006**, *128*, 6024–6025.
- (a) Santhosh, U.; Das, S. *J. Phys. Chem. A* **2000**, *104*, 1842–1847; (b) Arun, K. T.; Epe, B.; Ramaiah, D. *J. Phys. Chem. B* **2002**, *106*, 11622–11627; (c) Alex, S.; Basheer, M. C.; Arun, K. T.; Ramaiah, D.; Das, S. *J. Phys. Chem. A* **2007**, *111*, 3226–3230.
- (a) Goldsmith, C. R.; Lippard, S. J. *Inorg. Chem.* **2006**, *45*, 555–561; (b) Goldsmith, C. R.; Lippard, S. J. *Inorg. Chem.* **2006**, *45*, 6474–6478; (c) Kiyose, K.; Kojima, H.; Urano, Y.; Nagano, T. *J. Am. Chem. Soc.* **2006**, *128*, 6548–6549.
- Valeur, B. *Molecular Fluorescence: Principles and Applications*; Wiley-VCH: New York, NY, 2001; p 341.
- Ajayaghosh, A.; Arunkumar, E. *Org. Lett.* **2005**, *7*, 3135–3138.
- Zhang, X.; Xiao, Y.; Qian, X. *Angew. Chem., Int. Ed.* **2008**, *47*, 8025–8029.
- Keil, D.; Hartmann, H. *Dyes Pigm.* **2001**, *49*, 161–179.
- Lunelli, B. *Tetrahedron Lett.* **2007**, *48*, 3595–3597.